Mon. Not. R. Astron. Soc. **000**, 000–000 (0000) Printed 24 October 2016 (MN LATEX style file v2.2)

Scaling Laws of Passive-Scalar Diffusion in the Interstellar Medium

Matthew J. Colbrook,*[1] Xiangcheng Ma,[2] Philip F. Hopkins,[2] Jonathan Squire[2,3]

[1]*Department of Applied Mathematics and Theoretical Physics, University of Cambridge, Cambridge, CB3 0WA, UK*
[2]*TAPIR, Mailcode 350-17, California Institute of Technology, Pasadena, CA 91125, USA*
[3]*Walter Burke Institute for Theoretical Physics, Pasadena, CA 91125, USA*

Submitted to MNRAS, October 2016

ABSTRACT

Passive scalar mixing (metals, molecules, etc.) in the turbulent interstellar medium (ISM) is critical for abundance patterns of stars and clusters, galaxy and star formation, and cooling from the circumgalactic medium. However, the fundamental scaling laws remain poorly understood (and usually unresolved in numerical simulations) in the highly supersonic, magnetized, shearing regime relevant for the ISM. We therefore study the full scaling laws governing passive-scalar transport in idealized simulations of supersonic MHD turbulence, including shear. Using simple phenomenological arguments for the variation of diffusivity with scale based on Richardson diffusion, we propose a simple fractional diffusion equation to describe the turbulent advection of an initial passive scalar distribution. These predictions agree well with the measurements from simulations, and vary with turbulent Mach number in the expected manner, remaining valid even in the presence of a large-scale shear flow (e.g. rotation in a galactic disk). The evolution of the scalar distribution is not the same as obtained using simple, constant "effective diffusivity" as in Smagorinsky models, because the scale-dependence of turbulent transport means an initially Gaussian distribution quickly develops highly non-Gaussian tails. We also emphasize that these are mean scalings that only apply to *ensemble* behaviors (assuming many different, random scalar injection sites): individual Lagrangian "patches" remain coherent (poorly-mixed) and simply advect for a large number of turbulent flow-crossing times.

Key words: diffusion – ISM: evolution – methods: numerical – methods: analytical – stars: formation – galaxies: formation

arXiv:1610.06590v1 [astro-ph.GA] 20 Oct 2016

1 INTRODUCTION

Understanding transport processes in the interstellar medium (ISM) is crucial in the study of galaxy evolution, star formation and a wide range of observations in astronomy. For instance, observations of metal abundances in stars give us a window into the past history of galaxies such as our own Milky Way (Ivezić, Beers, & Jurić 2012), as well as mapping transitional epochs in the Universe such as the shift from Population III to Population II stars (Scannapieco, Schneider, & Ferrara 2003). In turn, these provide clues for how to formulate models for stellar enrichment and nucleosynthesis, star and star cluster formation, and even planet formation (Tremonti et al. 2004). However, because the ISM is turbulent, metals may mix on small spatial scales relatively easily – totally independent of how they are transported by bulk flows (e.g. galaxy inflows, mergers, outflows) or their original injection (via SNe or other stellar mass-loss processes). Such mixing may alter the interpretation of observations dramatically.

To first approximation, individual heavy-element species in the ISM can be treated as passive scalars (although they do participate in dynamics indirectly via cooling). Although passive scalar mixing in subsonic turbulence is well studied in the fluid dynamics community, turbulence in the ISM is highly supersonic (due to efficient radiative cooling) and magnetized. Further, the very large Reynolds numbers of $\sim 10^{10}$ or more (Fujita et al. 2003) are impossible to simulate directly. As such, it is important to understand some of the similarities and differences between mixing in neutral incompressible fluids, which tend to follow intuition based on terrestrial flows, and mixing in the supersonic magnetohydrodynamic (MHD) flows that are prevalent in the ISM. In this vein, Pan & Scannapieco (2010) have extended the subsonic Obukohov-Corrsin cascade phenomenology (Shraiman & Siggia 2000) to the compressible regime, showing that mixing time-scales are similar to the time-scales of kinetic energy dissipation, supporting the picture of a cascade of scalar fluctuations in supersonic turbulence. Other studies (e.g. Klessen & Lin 2003) have focused on a mixing length description and these ideas have had some success in simple diffusion models (e.g. Yang & Krumholz 2012). From such studies, it is clear that the mixing of metal tracers depends on the statistics of turbulence (which depend on parameters such as Mach number) and on the scale considered (in comparison to the physics driving the turbulence).

As such, an understanding of mixing in the ISM requires understanding the statistics of the supersonically turbulent velocity field. These can differ significantly from the velocity statistics in incompressible turbulence due to the formation of shocks, and "basic" properties such as the turbulent velocity scaling remain controversial. Due to this complexity, numerical simulations are key for testing ideas and simple phenomenological arguments. Recently, universal scaling laws for the mass-weighted turbulent velocity have been proposed (Kritsuk et al. 2007a,b) and tested in a number of numerical studies (Kowal & Lazarian 2007a,b; Schmidt et al. 2008; Federrath et al. 2010; Price & Federrath 2010; Schwarz et al. 2010). Some analytic scaling relations for velocity have also been proposed (Falkovich et al. 2010; Galtier & Banerjee 2011; Wagner et al. 2012; Banerjee & Galtier 2013). These are discussed in Kritsuk, Wagner, & Norman (2013) with an analysis analogous to the Kolmogorov picture of an energy cascade. As well as being important for mixing, these scalings are fundamental inputs to modern theories of star formation via "turbulent fragmentation" (Pan, Padoan, & Kritsuk 2009; Hopkins 2013).

Due to the very high Reynolds numbers, most studies are

* E-mail:mjc249@cam.ac.uk

forced to adopt a Subgrid-Scale Model (SGS) to simulate ISM mixing, since it is not possible to resolve the viscous scale (but see, for example, Petit et al. 2015). A popular example is the Smagorinsky (1963) model, which adopts a locally-constant eddy diffusivity proportional to the resolved strain rate tensor. Shen, Wadsley, & Stinson (2010) found that such subgrid feedback models alter the metal enrichment in smoothed-particle hydrodynamics (SPH) simulations significantly. However, this model fails to describe the scale-dependence of turbulence; moreover, it was derived for highly subsonic, nonmagnetized turbulent flows, without bulk velocity shear – none of these assumptions hold in the ISM. As highlighted by Wadsley, Veeravalli, & Couchman (2008), using these simple scalings without a more physically-motivated formulation of dissipation can lead to order-of-magnitude errors, and even their qualitative "correctness" and convergence may not be well defined.

In this paper we seek to study the local diffusion properties of a passive tracer initially "injected" into a super-sonically MHD turbulent medium, with and without a background shear flow. Following the above discussion, we investigate the possibility of a scaling law for the diffusivity that is dependent on wavenumber/length scale, in a similar manner to *Richardson diffusion* in subsonic flows (Richardson 1926). We ignore the details of radiative cooling and heating and instead make the common simplification of treating the ISM with an approximately isothermal equation of state. We also ignore self-gravity (because we do not wish to explicitly follow star formation). The results can be viewed as an extension of Klessen & Lin (2003) and of Richardson diffusion into the highly-compressible supersonic regime. While there have been arguments for describing anomalous diffusion in this way in other physical situations (Stanislavsky 2010; Metzler & Klafter 2000; Balescu 1995; Balakrishnan 1985), so far as we know this is the first time such a model has been tested against numerical data for supersonic MHD turbulence, as relevant to transport in the ISM. We shall argue that Richardson's scaling for a diffusivity $D(l) \propto \epsilon^{1/3} l^{4/3}$, where ϵ is the mean energy dissipation, becomes steeper in supersonic MHD flows due to the different scaling of the velocity structure functions. More concretely, we argue that within an inertial range of wavenumbers, the process can be described by a *fractional diffusion* process, with $\partial_t \widehat{\theta}(\mathbf{k}) = -|\mathbf{k}|^2 \kappa(\mathbf{k}) \widehat{\theta}(\mathbf{k})$ with $\kappa \propto \mathcal{M}|\mathbf{k}|^{-\alpha}$ and $\alpha \sim 1+\zeta(1)$. Here θ denotes metal density, $\mathcal{M}$ Mach number and $\widehat{x}$ denotes the Fourier transform of x. Such a model agrees well with our MHD simulations in two and three dimensions, at various Mach numbers and in the presence of a shear (simulating rotation of a galactic disc).

The paper is organized as follows: in § 2, we outline the theory of classical mixing length descriptions and our argument; § 3 describes our method and simulations; results and comparison with theory are discussed in § 4; our conclusions and the implications for metal transport in the ISM are outlined in § 5.

2 THEORY

We do not give a full account of the statistics of mixing in supersonic turbulence and refer the reader to papers such as Pan & Scannapieco (2010) for such a treatment where the classic picture of a cascade of scalar fluctuations is applied to the supersonic regime. Crucially, in agreement with our argument below, it was found there (and in subsequent studies) that, for a wide range of Mach numbers, the mixing time-scale was proportional to the turnover time of eddies at the length scale of the scalar sources. Here we consider the simple case where a tracer is "released" in an initially highly-concentrated (δ-function or "point source") distribution around an injection site, and attempt to follow its "diffusion."

Taylor (1922) introduced the formula

$$\frac{\mathrm{d}}{\mathrm{d}t}\xi = \int_0^t \left\langle \mathbf{v}(\mathbf{x}(0),0)\cdot\mathbf{v}(\mathbf{x}(t'),t')\right\rangle \mathrm{d}t' \tag{1}$$

where $\xi = \langle|\mathbf{x}(t)-\mathbf{x}(0)|^2\rangle$ is the ensemble average of particle displacements following a Lagrangian trajectory and $\mathbf{v}$ denotes an Eulerian velocity. Conceptually, this links the statistics of the Lagrangian and Eulerian viewpoints. In the above, we assume isotropy so that ξ need not be defined for different directions (this does not have to be true in MHD turbulence, but we will show below it is valid in an *ensemble* sense). For times much larger than the autocorrelation time, τ, we expect the right-hand side to be a constant and hence the left-hand side gives a definition of a Lagrangian diffusivity, $D = \mathrm{d}\xi/\mathrm{d}t$.

If $f(\mathbf{r},t)$ denotes the probability distribution for finding a particle (or element of tracer) at position $\mathbf{r} \equiv \mathbf{x}(t)-\mathbf{x}(0)$ after a time t then, *if we assume* the position has a Gaussian distribution (corresponding to a first-order Markov process or random walk, see Sawford 2001), we expect (following Batchelor 1949) a diffusion equation to hold:

$$\partial_t f = D\nabla^2 f. \tag{2}$$

In a real turbulent flow in the inertial range, the assumption of Gaussian statistics is far from correct. If we consider turbulence as a hierarchy of eddies, we can attach to each eddy a length scale $\hat{l}$ and a velocity scale $\hat{v}$. These determine the eddy turnover time as $\hat{\tau} = \hat{l}/\hat{v}$. For $t < \hat{\tau}$ individual elements (molecules, metal species, etc.) which are "injected together" are strongly correlated, which leads to the estimate $|\mathbf{x}(t)-\mathbf{x}(0)| \approx \hat{v}t$ and $D(t) \approx 2\hat{v}^2 t$. This is simply the ballistic motion – pure advection at a locally constant velocity – of a tracer in the eddy's local flow. For $t \gg \hat{\tau}$ the eddy has dispersed and destroyed the correlation in the velocity field, implying we should replace t by $\hat{\tau} = \hat{l}/\hat{v}$, and giving the estimate $D(t) \approx 2\hat{l}\hat{v}$ for the diffusion coefficient. Hence the expected scalings are

$$D(t) \approx \begin{cases} 2\hat{v}^2 t, & t < \hat{\tau} \\ 2\hat{l}\hat{v}, & t \gg \hat{\tau} \end{cases} \tag{3}$$

For our purposes, note the shift of scale dependence on $\hat{v}$ and the scale dependence of the diffusion constant for $t \gg \hat{\tau}$. Klessen & Lin (2003) found that this approach can be continued into the compressible regime by introducing a shock travel length l^* and rms velocity v^*, leading to the crossing time $\tau^* = l^* v^*$. They used $l^* = L/k_f$, where L is the size of the region under consideration and k_f the forcing wavenumber for their numerical simulations. We now extend these ideas by studying the analogous scalings of D for a range of wavenumbers, not just those which contain the most energy.

Similar arguments to those described in the previous paragraph were originally proposed by Richardson (1926), who suggested that dispersion of nearby particles (two-point statistics) is diffusive with $D \sim r^{4/3}$. This is usually stated in the form $\langle r^2(t)\rangle \sim \epsilon t^3$ (here, $\langle r^2(t)\rangle$ denotes the mean square particle separation and ϵ the energy dissipation rate). The physical argument is that, in the inertial range, only eddies with a scale similar to the particle separation act to increase the separation. For, say, a "patch" or concentration of scalar density with some physical scale, much smaller eddies simply stir scalars *within* the patch, while much larger ed-

dies simply advect the entire patch. As the separation ("patch size") increases, it encounters "resonant" eddies of increasing size and hence diffuses faster. The scaling of eddies with physical scale is quantified in terms of structure functions (e.g. Monin & Iaglom 1975), which are defined by

$$S_p(l) \equiv \langle |\mathbf{v}(\mathbf{x}+|\mathbf{l}|) - \mathbf{v}(\mathbf{x})|^p \rangle \, , \tag{4}$$

where $\langle \cdot \rangle$ is the ensemble average and $l = |\mathbf{l}|$; i.e., we assume the turbulence is isotropic. For large Reynolds numbers turbulence is scale-free (far from the energy injection and dissipation scales), and thus the structure functions must satisfy the power law scaling $S_p(l) \sim l^{\zeta(p)}$.

The standard subsonic Kolmogorov scaling gives $\zeta(p) \approx p/3$, which has been supported with experimental data for small p. If we take the regime where $D \sim \hat{l}\hat{v}$ and $\langle \Delta_l \hat{v} \rangle \sim l^{\zeta(1)}$ then we obtain $D \sim l^{1+\zeta(1)} \sim l^{4/3}$ in agreement with Richardson's scaling. For the regime $t < \hat{\tau}$ we obtain $D \sim l^{\zeta(2)} t$ and Kolmogorov gives $\zeta(2) = 2/3$. In summary, if we assume for large Reynolds numbers turbulence relaxes into a self-similar state with fluctuations obeying Eq. (4), then upon taking ensemble averages of Eq. (3) it is reasonable to expect

$$D \sim \begin{cases} l^{\zeta(2)} t & t < \hat{\tau} \\ l^{\zeta(1)+1} & t \gg \hat{\tau} \end{cases} . \tag{5}$$

The velocity structure function scalings of supersonic turbulence differ from those in subsonic turbulence. A common estimate in the supersonic cascade is $\zeta(1) \approx 0.5$, perhaps increasing slightly as Mach number is increased. The value for $\zeta(2)$ is less well known but should be in the range $\zeta(2) \sim 0.8 - 1$. The main difficulty in testing these numerically is the large Reynolds number required to gain a large enough inertial range (Gioia et al. 2004), particularly in supersonic turbulence where one must also be above the scales at which the flows become subsonic.

Since the diffusion process described in Eq. (5) explicitly depends on the scale being considered, it is most natural to consider the diffusion of the tracer in the Fourier domain:[1]

$$\partial_t \widehat{\theta}(\mathbf{k}) = -k_i \, \kappa_{ij}(\mathbf{k}) \, k_j \, \widehat{\theta}(\mathbf{k}). \tag{7}$$

Here and throughout, θ denotes the passive scalar (e.g. metal) density profile. In isotropic turbulence, we may take $\kappa_{ij} = \kappa \, \delta_{ij}$ and if we assume a power law scaling (i.e., scale invariance of the turbulence) $\kappa(k) \propto k^{-\alpha}$ (with $k \equiv |\mathbf{k}|$) then Eq. (7) corresponds to $\partial_t \theta = -(-\Delta)^{(2-\alpha)/2} \theta$, i.e. a fractional derivative. Letting $\beta = 2 - \alpha$, the case $\beta = 2$ corresponds to a standard diffusion equation. In the case of $0 < \beta < 2$ we obtain the evolution equation for the probability distribution function of a stable[2] Lévy flight (Klages, Radons, & Sokolov 2008). This extends the standard diffusion model to situations where assumptions of locality, Gaussianity and lack of long-range correlations fail to hold. A similar model has met with some success for the description of transport in plasma turbulence (del Castillo-Negrete, Carreras, & Lynch 2005).

[1] Working in n dimensions we define the Fourier transform of a function f with domain $\Re^n$ as

$$\widehat{f}(\mathbf{k}) = \int_{\Re^n} f(\mathbf{x}) \exp(-i\mathbf{x}\cdot\mathbf{k}) \, \mathrm{d}\mathbf{x}. \tag{6}$$

[2] This means that the probability density of any linear combination of uncorrelated random variables with this distribution coincides with the original distribution up to rescaling.

Taking $\kappa = k^{-\alpha}$, the solution of Eq. (7) with an initial point source is

$$\theta(r,t) = \frac{1}{(2\pi)^n} \int_{\Re^n} \exp(i\mathbf{k}\cdot\mathbf{x} - k^\beta t) \, \mathrm{d}\mathbf{k} \sim \frac{t}{r^{n+\beta}} \sim \frac{t}{r^{2+n-\alpha}} \tag{8}$$

for large $r = |\mathbf{r}|$, where n is the dimension of the system. Using this, it is easy to see that the fractional moments $\langle r^\delta \rangle$ diverge for $\delta \geq \beta$. However, for $0 \leq \delta < \beta$ we have

$$\langle r^\delta \rangle \sim t^{\frac{\delta}{\beta}} \tag{9}$$

and one can extend this scaling to larger δ by accounting for cut-off effects (Metzler & Klafter 2000). Taking $\beta = 2 - \alpha = 1 - \zeta(1)$ gives a prediction which agrees with Richardson's scaling $\langle r^2(t) \rangle \sim \epsilon t^3$ (albeit for single-particle separation), while for supersonic turbulence with the estimate $\zeta(1) \approx 1/2$ we obtain $\langle r^2 \rangle \sim t^4$. Similarly, for small k we may expect $\kappa \propto k^{-\zeta(2)} t$, and so both scalings become steeper as we increase the Mach number.

The considerations of the previous paragraph suggest that we should be able to *measure* a well-defined, scale-dependent "diffusivity" by measuring

$$\kappa = -\frac{\partial_t \widehat{\theta}}{k^2 \widehat{\theta}} \tag{10}$$

from numerical simulations. This is consistent with the classical case with constant diffusion coefficient and has the advantage of being straightforward to compute numerically. If we take the scalings in Eq. (5) then one may conjecture that

$$\kappa = A \mathcal{M} k^{-\alpha} \tag{11}$$

within the inertial range of wavenumbers.

3 DIRECT NUMERICAL SIMULATIONS

3.1 Code and Turbulent Driving

The simulations here were run with GIZMO[3] (Hopkins 2015b), a mesh-free Lagrangian finite-volume Godunov code, in its Meshless-Finite Mass (MFM) mode. This method is designed to capture advantages of both smoothed-particle hydrodynamics (SPH) and grid-based adaptive-mesh refinement (AMR) methods. The advantages of the method are described and tested in extensive detail with a survey of ~ 100 test problems in Hopkins (2015b); Hopkins & Raives (2015); Hopkins (2015a), for both hydrodynamics and MHD, demonstrating good accuracy and agreement with well-studied regular-grid and moving-mesh Godunov codes. Of particular relevance to our studies here, these include both subsonic and super-sonic MHD turbulence tests.

In all cases considered in this paper, the turbulent driving routines, including parameters, follow Bauer & Springel (2012). The usual box stirring method (e.g. Schmidt, Federrath, & Klessen 2008; Federrath, Klessen, & Schmidt 2008; Price & Federrath 2010) is employed, with a small number of modes (wavelengths 1/2 to 1 times the box size) driven in Fourier space as an Ornstein-Uhlenbeck process, with the compressive part of the acceleration projected out via a Helmholtz decomposition in Fourier space so that the driving is a "natural" mix of equal parts compressible and incompressible/solenoidal modes. We initialize a uniform seed field $\mathbf{B} = B_0 \hat{z}$; the seed field is chosen to have a trace initial value so that

[3] A public version of the code, including all physics and numerical methods used in the simulations here, is available at: http://www.tapir.caltech.edu/~phopkins/Site/GIZMO.html

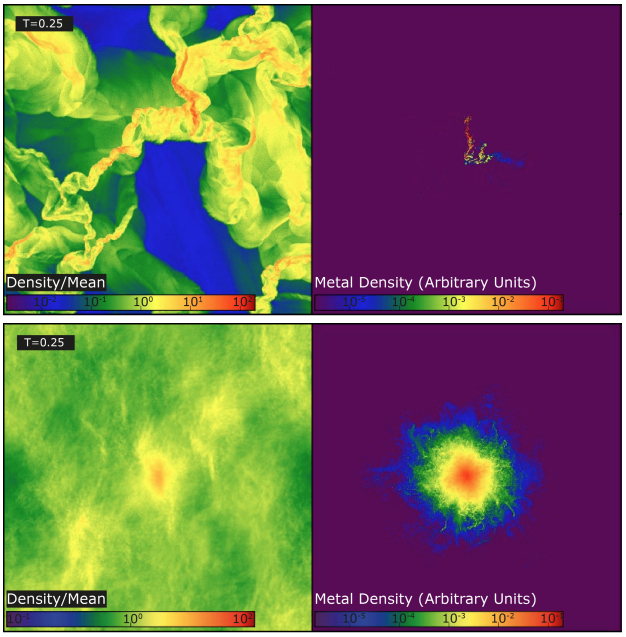

Figure 1. *Top:* Gas density ρ (*left*) and passive scalar/metal density θ (*right*), denoted by color (as labeled), in one of our simulations (the 2D shearing-box). We show all quantities directly "as they are" in the code at a time $t = 0.25$ (in code units; a few crossing times at the initial injection scale) after a single point-like "injection" of the metals/scalars into the center of the box. Clearly, the distribution even after a few small-scale turbulent crossings is highly anisotropic, dominated by advection and shear along field lines – it does not resemble diffusion. *Bottom:* Same, but repeating the "injection" process at 80 different random locations in the box, each at 15 different random initial times (1200 injections in total), then averaging all of the resulting maps together (after re-centering each on the center of the tracer mass distribution). The is the "averaged" profile $\theta(r,t)$ that we analyze. In *ensemble-average*, the distribution is both isotropic (despite shear and magnetic fields being present) and qualitatively diffusion-like.

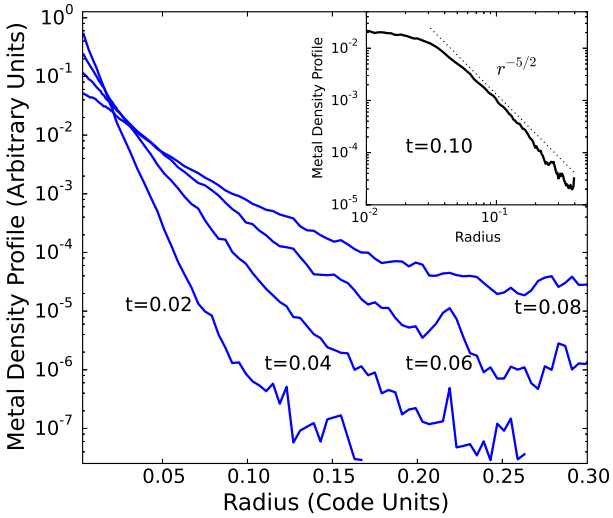

Figure 2. The ensemble-averaged metal density profile $\theta(r,t)$ at time t after tracer release (in our 2D, non-shearing, $\mathcal{M} = 5$ simulation, but all other simulations are qualitatively similar). A scale-independent "effective diffusivity" κ would produce a Gaussian profile here ($\theta \propto \exp[-Cr^2]$; this would appear as a parabola in the main figure), but this is not a good description of the profile at *any* time shown, especially in the "tails." The inset shows the profile at the final time $t = 0.1$ in log-log space, demonstrating that the tails have a clear power-law behavior. We compare the analytically predicted power-law slope (§ 4.1) from our theoretical model of scale-dependent diffusion ($\theta \propto r^{-5/2}$); this agrees well with the simulations.

it is self-consistently amplified to saturation values by the turbulence (we do not consider cases with a strong mean-field such that the turbulence would be sub-Alfvenic, as this is not believed to occur in the situations of interest in the ISM). We discard all simulation outputs until all turbulent properties have reached a statistical steady-state (after the first few crossing times).

Our simulation with shear uses the standard shearing-sheet approximation (see Guan & Gammie 2008). We solve the azimuthally-symmetric equations (following cylindrical R, z coordinates) in a frame which co-rotates with circular orbits, with frame-centered orbital frequency Ω. This amounts to adopting shear-periodic boundary conditions with centrifugal and Coriolis accelerations $\mathbf{a} = 2qx\Omega^2\hat{x} + 2\mathbf{v}\times(\Omega\hat{z})$ (where $q \equiv -d\ln\Omega/d\ln R = 1$ here, for a constant-circular velocity disk).

3.2 Conventions and Units

We briefly summarize conventions used. The wavenumber $k = |\mathbf{k}|$ defines a "length" scale $\ell = 2\pi/k$. We adopt an isothermal equation of state ($\gamma = 1$) for the gas which is reasonable for the density and temperature ranges considered (given efficient cooling in the real ISM) and enables comparison with the "standard" ISM turbulence literature. Due to the scale-free nature of the MHD equations (and the choice to have a negligible mean magnetic field; see below for further discussion), our results are entirely determined by the dimensionless Mach number (Hopkins & Lee 2016). We set the sound speed c_s, box length $L_{\rm box}$ and box mass $M_{\rm box}$ to unity in code units and define the Mach number $\mathcal{M} \equiv \langle v_t^2\rangle^{1/2}/C_s$, where $\langle v_t^2\rangle^{1/2}$ is measured at the box-scale.

3.3 Runs Performed

For the non-shearing cases we consider a (1) 3D box, $\mathcal{M} = 2$, (2) 3D box, $\mathcal{M} = 10$, (3) 2D box, $\mathcal{M} = 5$. We also consider (4) a 2D shearing case, $\mathcal{M} = 2$, where we take $\Omega = 10$, so the velocity scale-height $H \equiv \sqrt{c_s^2 + v_t^2}/\Omega \approx 0.2$ (the turbulent driving scale is automatically set to $= H$, appropriate for the driving scale being the disk scale-height in a stratified disk). 3D (2D) simulations use 256^3 (1024^2) particles.

For weak mean-field cases of interest here the Mach number $\mathcal{M}$ also determines the saturated volume-averaged Alfvén Mach number $\mathcal{M}_A = \langle|\mathbf{v}|/v_A\rangle$, where the Alfvén speed $v_A = |\mathbf{B}|/\rho^{1/2}$. We find $\mathcal{M}_A \approx 5$ at saturation in all cases, i.e. $\sim 5\%$ of the turbulent kinetic energy in magnetic fields, consistent with standard numerical studies (Kritsuk et al. 2011; Federrath et al. 2014) and simple analytic expectations (Brandenburg & Subramanian 2005) of amplification via the supersonic turbulent dynamo.

3.4 Tracer Analysis

Particle identities are stored throughout the simulation. Consider a single trial (denoted α); in this trial each particle is assigned an initial scalar field $Z_n^{(\alpha)}$ (Z for metallicity). We can then trace the particle, reconstruct their transport, and repeat the "injection" in a new trial α', with little computational effort. The tracer concentration (or metal density) for each trial, $\theta^{(\alpha)}$, can be determined via projection onto a fixed grid as

$$\theta_{ijk}^{(\alpha)}(\mathbf{x},t) = \sum_{\rm particles\, n} m_n Z_n^{(\alpha)} W(\mathbf{x}_{ijk} - \mathbf{x}_n(t), h_{ijk}) \quad (12)$$

where m_n is the mass of the nth particle, i,j,k index the grid cells (with positions $\mathbf{x}_{ijk}$) in three dimensions, and W denotes a cubic

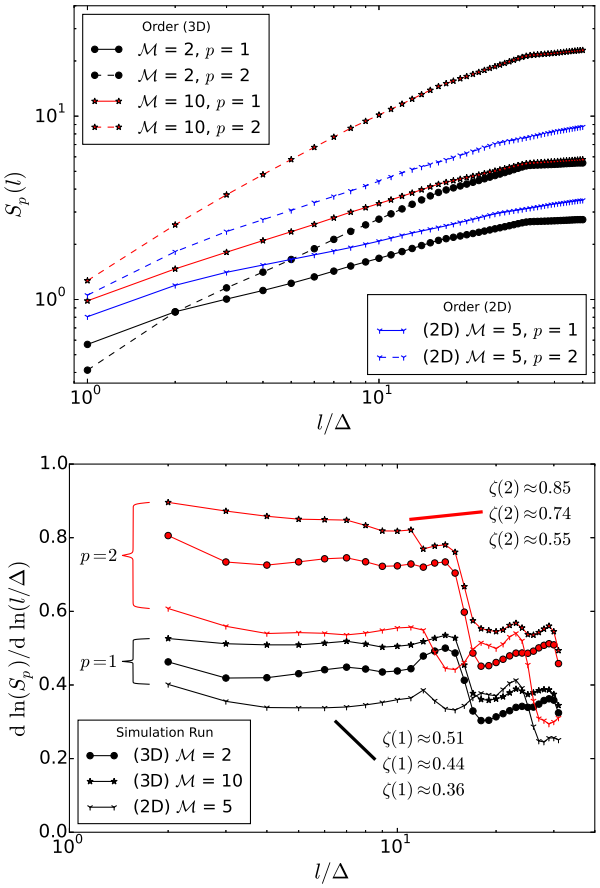

Figure 3. *Top:* Structure functions $S_p(l) \equiv \langle |v_t(x+l) - v_t(x)|^p \rangle$ (scalings of the turbulent gas velocity field with spatial scale; Eq. 4), of order $p = 1, 2$ for our non-shearing simulations. Δ is the grid spacing. *Bottom:* Power-law slope of the structure functions above: this defines the exponents $\zeta(p)$ via $S_p(l) \propto l^{\zeta(p)}$. The inertial range is the regime where $\zeta \approx$ constant (S_p is a power-law); at large l the box-scale boundary conditions and driving corrupt the scaling (and we choose Δ so that scales $l < \Delta$ are not well-resolved). For super-sonic turbulence we expect $\zeta(1) \sim 0.5$ and $\zeta(2) \sim 2/3 - 1$, both weakly increasing with Mach number, as found here (the 2D case is noticeably lower, although similar to values seen in other studies at this Mach number and dimensionality).

spline interpolant (see Springel 2011), where h_{ijk} is a spline kernel length adapted to enclose the nearest ~ 64 particles around each grid cell center (our results are not sensitive to this choice). We project onto a 1024^2 grid in two dimensions and onto a 256^3 grid in three dimensions.

The initial density is chosen to be a strongly peaked Gaussian with standard deviation 0.005 in code units. The choice of standard deviation does not effect the scaling of κ but is chosen to allow a large number of times to be sampled before the size of the tracer cloud becomes comparable to the size of the box.

We wish to capture the evolution of θ and work in a local frame where $\overline{\mathbf{u}} = 0$ to ignore simple bulk advection. The fact that the tracer is highly localized and the use of periodic boundary conditions allows us to average over space by positioning the centre of the Gaussian at different points (for each trial) and taking the average of the field at each time step. In all cases, we consider $N_{\rm trials} = 1200$ trials, where we take 15 different initial "injection times," each with 80 different "injection locations." For cases without shear the injection centers are randomly positioned anywhere in the box, whereas for the sheared case we sample from a plane tangential to the direction of background flow. At each time t, we center the grid on the center of the scalar field (which corrects for local advection and aims to capture the diffusion process in the Lagrangian frame of the mean velocity). We can then define the ensemble average:

$$\theta_{ijk}(\mathbf{x},t) = \frac{1}{N_{\rm trials}} \sum_{\alpha=1}^{N_{\rm trials}} \theta_{ijk}^{(\alpha)}(\mathbf{x},t) \quad (13)$$

Finally we average this in radial shells $r \equiv |\mathbf{x}|$, to obtain a radial profile $\theta(r,t)$. At long times after injection, when the profile/scalar distribution scale length becomes comparable to the box size, the periodic boundary conditions artificially corrupt further evolution, so we consider only those times before the profile has been distorted by the edge of the box.

To calculate $\widehat{\theta}$ we numerically compute

$$\widehat{\theta}(\mathbf{k},t) = \int_{\Re^n} \theta(r,t) \exp(-i\,\mathbf{r}\cdot\mathbf{k})\, d\mathbf{r}, \quad (14)$$

using the radially averaged $\theta(r,t)$. We then approximate the time-derivative using a finite-difference

$$\partial_t \widehat{\theta} \approx \frac{\widehat{\theta}(k,t+\Delta t) - \widehat{\theta}(k,t-\Delta t)}{2\Delta t} \quad (15)$$

for $\Delta t = 0.005$, to allow computation of the diffusivity Eq. (10).

4 RESULTS

4.1 Scalar Density Distributions: Simple, Constant Diffusivity Cannot Describe the Simulations

As an illustrative example of our passive-scalar tracing procedure, Fig. 1 shows the evolution of one tracer injection/release, and compares it to an ensemble average over ~ 1200 tracer releases randomly distributed in the turbulence in both space and time. One can see that for an *individual* injection, after a time ~ 0.25 (a few eddy turnover times for eddies with length of order the initial injection spatial scale), the dominant term is simply advection, with some shearing and distortion of the Lagrangian "parcel" of gas. The distribution does not, in any meaningful sense, resemble the solution to a diffusion equation. However, when we *ensemble-average*, the distribution shows behavior much more similar to our expectations for diffusive processes. The distribution is approximately radially symmetric about the injection site – i.e. there is no ensemble-average preferred direction imposed either by local advection or magnetic fields – expected on sufficiently large scales owing to our weak mean-field assumption but not guaranteed on small scales – and the distribution falls off radially in diffusion-like manner.

Fig. 2 shows the ensemble-averaged scalar density profiles $\theta(r,t)$ for one of our simulations (all show the same qualitative behavior). Although the initial profile of the injected tracer is, by construction, Gaussian, the profile develops thicker, highly non-Gaussian "superdiffusive" tails rapidly. If the "effective diffusivity" were scale-independent ($\kappa = $ const) then Eq. (7) would give the standard Gaussian diffusion solution: $\theta(r,t) \propto \exp[-r^2/4t\kappa]$. However, recall in § 2, Eq. (8) we showed that if $\kappa \propto k^{-\alpha}$, then $\theta(r,t) \propto t\, r^{-(2+n-\alpha)}$ where n is the dimension of the system and $\alpha \approx 3/2$ (for supersonic turbulence). This gives $\theta(r,t) \propto r^{-5/2}$ in 2D and $\propto r^{-7/2}$ in 3D, agreeing nearly perfectly with the behavior in the simulations. This illustrates that the process is well described by a fractional diffusion with the scaling expected from supersonic turbulence. However, the long times that are required for

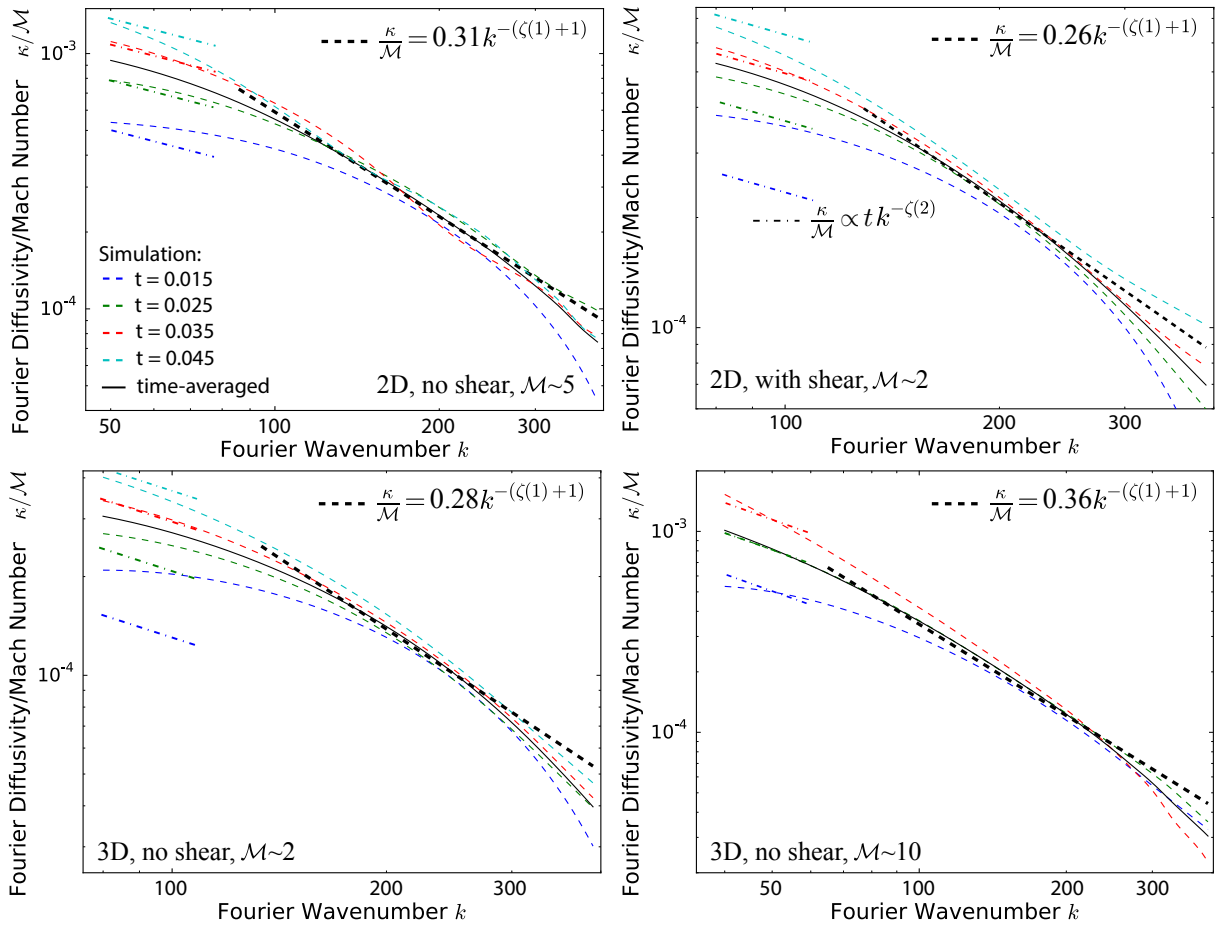

Figure 4. "Fourier Diffusivity" κ as a function of k (effective diffusivity of modes with wavenumber k, defined as $\kappa \equiv -\partial_t\widehat{\theta}/(k^2\widehat{\theta})$, see §2), normalized by the box Mach number $\mathcal{M}$. We plot this at different times and the mean over all times sampled (as labeled), for each of our four simulations (each panel). We compare our theoretical prediction from Eq. 5 and Eq. 11, for both the inertial range where we expect a time-independent scaling $\kappa/\mathcal{M} = Ak^{-(\zeta(1)+1)}$ (Eq. 11; thick-dashed lines), and for small k, where we expect a time-dependent scaling $\kappa/\mathcal{M} \propto tk^{-\zeta(2)}$ (Eq. 5; dot-dashed lines). For each case we use the ζ values directly measured for the same simulation in Fig. 3. The analytic scalings agree remarkably well with the simulations. In the inertial range from Fig. 3, we confirm a time-independent scaling with universal constant coefficient $A \approx 0.3$, independent of Mach number, dimensionality, shear, and magnetic field strength. This corresponds to the simple physical scaling $\kappa \sim v_t(\ell)\,\ell \sim k^{-1.5}$ in real-space. At small-k, the scaling is dominated by simple "ballistic motion" of Lagrangian gas elements; this agrees very well at $\mathcal{M} \sim 5-10$, however for small $\mathcal{M}$, the time-dependence appears weaker than our simple prediction ($\kappa \propto t^{1/2}$ rather than $\propto t$).

true power-law tails to develop also serve to highlight the difficulty in estimating the diffusivity κ. By the time the tails develop the asymptotic scaling, the tracer has begun to diffuse to the boundary of our box.

4.2 Fourier Scalings: How Does Diffusivity Depend on Scale?

For comparison with the simple theory outlined in §2 we must first estimate the structure functions of the gas velocity distributions, which is carried out using the grids described above. We calculated the transverse structure functions (i.e., taking $\mathbf{l}$ perpendicular to the velocity component), since previous works suggest that these should show more robust scaling (Boldyrev, Nordlund, & Padoan 2002). Fig. 3 shows the structure functions for $p = 1,2$ plotted against l/Δ, where Δ is the grid spacing. Fig. 3 shows the local gradient, which gives an estimate for $\zeta(p)$. There is an an inertial range of values of l for which a clear scaling is evident. Taking the average over this range we find $\zeta(1) \approx 0.36, \zeta(2) \approx 0.55$ in 2D at $\mathcal{M} \sim 5$, $\zeta(1) \approx 0.44, \zeta(2) \approx 0.74$ in 3D at $\mathcal{M} \sim 2$ and $\zeta(1) \approx 0.51, \zeta(2) \approx 0.85$ in 3D at $\mathcal{M} \sim 10$. In general, the exponents $\zeta(p)$ are not universal and depend on Mach number and how the turbulence is driven. As expected, the ζ values increase (weakly) with Mach number (scalings become steeper), as the turbulence becomes more strongly shock-dominated (Kritsuk et al. 2013). The measured structure functions are consistent with previous results, although perhaps somewhat low for the 2D simulation.

We now calculate the "Fourier Diffusivity" (effective diffusivity associated with modes of wavenumber k) $\kappa = -\partial_t\widehat{\theta}/(k^2\widehat{\theta})$, as described in § 2. This is done as a function of k, at different times t, with the results for each of our simulations shown in Fig. 4. There is a clear region associated with the same inertial scale where the diffusivities coincide independent of time. We overplot the expected power-law scalings from our theory and the measured structure functions (Eq. 5). The agreement is remarkable. In the inertial range, the time-independent power-law agrees well with our analytic scaling of the form in Eq. 11 ($\kappa \sim A\,\mathcal{M}\,k^{-(\zeta(1)+1)}$), with a

time-independent normalization $A \approx 0.3$ which appears universal in our simulations (independent of Mach number, dimensionality, and shear). Deviations from this at the largest k owe to (1) limited numerical resolution, and (2) approaching the sonic scale (below which the turbulence becomes sub-sonic). At small k, we transition to "ballistic motion" dominating the transport, with expected scaling $\kappa \sim t\,k^{-\zeta(2)}$. Here the power-law scaling agrees very well with the simulations and the normalization increases with time as expected; however, while the predicted (linear) dependence on time agrees extremely well with our $\mathcal{M} = 5-10$ runs it appears too strong for our $\mathcal{M} = 2$ runs. It appears that as the Mach numbers become smaller (trans-sonic here), the motion cannot be considered purely "ballistic" (perhaps because of pressure forces) but a slower scaling $\propto t^{1/2}$ (suggesting incoherent addition of eddies) applies.

Comparing 2D and 3D cases, the qualitative features are exactly the same, and the agreement with the theory remains very good, despite the fact that the cascade and structure function scalings are different in 2D. This may owe in part to the fact that we focus on super-sonic turbulence, where the 2D/3D differences are smaller. The scaling of κ is slightly steeper as we increase $\mathcal{M}$, but this is exactly as expected if it scales with ζ as measured in the simulations. Note that for $\mathcal{M} \sim 10$, we show a reduced number of times because the increased Mach number leads to the pollution of the measurement by the box boundary at earlier times. In the shearing case, we also see similar results. At large k this may be expected, since the shear velocity $\Delta v_{\rm shear} \sim \Omega\ell$ is sub-dominant to the turbulent velocities below the velocity scale-length $H = (c_s^2 + v_t^2)^{1/2}/\Omega \approx 0.2$ (defined above). By the time the diffusion expands beyond these scales, it is directly influenced by the boundary conditions (but in any case, the shearing-box approximation is no longer valid on scales $\gg H$). So we caution that our "with shear" results are *not* necessarily valid in the regime where shear *dominates* the motion, but only when it is present but secondary to turbulence. Nonetheless, it is significant on the small scales – it causes an "aliasing" (slight elliptical distortion of the "diffusion radius") if we do not properly account for it, which we do by transforming the y coordinate to $Y = y + Stx$ (factoring out the linearized "pure shear" motion on our initial tracer injection, so we can consider the truly diffusive component).

5 CONCLUSIONS

We have developed an analytic theory for, and tested in direct numerical simulations, the diffusion of passive scalars in two and three dimensional super-sonic, magnetized, isothermal turbulence, with and without an external shear field. We summarize our conclusions as follows:

(i) We show that the "effective diffusivity" κ cannot be constant, i.e. the scalar density does not obey a pure diffusion equation $\partial_t Z = \kappa \nabla^2 Z$, with $\kappa = $ constant. This would conserve a Gaussian-like profile; however, if we inject tracers to follow their evolution, we see large non-Gaussian tails appear immediately, indicating that κ must be scale-dependent.

(ii) We demonstrate the existence of an effective time-independent scale-dependent diffusivity $\kappa(k)$, which explains the non-Gaussian features and time-dependence described above, and is invariant over a suitable range of scales $\ell = 2\pi/k$ (corresponding to the inertial range). This scaling is approximately given (in both 2D and 3D) by:

$$\kappa \approx 0.3 \mathcal{M}_{L_{\rm box}} (k L_{\rm box})^{-\alpha} \quad (16)$$

where $\mathcal{M}_{L_{\rm box}} = \mathcal{M}(L_{\rm box}) = \mathcal{M}$ is the Mach number (defined at some normalization scale, here the box scale $L_{\rm box}$) and the scaling exponent α increases weakly from ≈ 1.44 at Mach numbers $\mathcal{M} \sim 2$ to ≈ 1.51 at Mach numbers $\mathcal{M} \sim 10$. In other words, the system can be modeled as a diffusion process, but with each mode of the tracer density field obeying a separate diffusion equation according to its mode-dependent diffusivity.

(iii) The exponents α agree well with arguments based on the velocity structure functions of the turbulence in the inertial range. Dimensionally, if eddies of scale ℓ advect or mix material on their crossing time, we expect a scaling of $\kappa \sim v_t(\ell)\ell$, where $v_t(\ell) \propto \ell^{\zeta(1)}$ is the characteristic eddy velocity on scales ℓ. Based on the phenomenology of supersonic turbulence, we expect $\zeta(1) \sim 0.5$, possibly increasing with Mach number (see Kowal & Lazarian (2007a,b); Schmidt et al. (2008); Federrath et al. (2010); Price & Federrath (2010); Schwarz et al. (2010)), giving $\kappa \sim \ell^{1.5}$. This is almost exactly what we measure directly, including the weak dependence on Mach number, which indicates the validity of the simple phenomenological arguments.

(iv) We identify a superdiffusive regime at large scales and small times, where the eddies simply transport the particles via bulk advection ("ballistic motion"), leading to the scaling

$$\kappa \propto t\,\ell^{\zeta(2)}. \quad (17)$$

(v) We demonstrate that these statements are only valid in a statistical, *ensemble-averaged* sense: any individual Lagrangian parcel of fluid can be distorted into a high non-symmetric shape which bears no resemblance to the isotropic solution of a diffusion equation, and can remain coherent for many turbulent crossing times. Diffusive behavior only appears after ensemble-averaging over all possible behaviors. This has important implications for physical systems: for e.g. metal mixing, it means that "metal diffusion" only applies when the number of "sources" is large and well-distributed in time and/or space. If we consider the material injected by e.g. just a single SNe explosion (or, on larger scales, the SNe from a single star cluster), which may be very important for the second-generation of star formation, this material does not simply diffuse but may create long-lived "pockets" of enriched gas.

(vi) We show that our scalings above remain true in the presence of a coherent shear force – at least on scales where the shear velocity is sub-dominant to the turbulent motions – once the simple shear has been accounted for in the tracer profile. Clearly, more study of the shearing case is warranted to develop fundamentally anisotropic scalings that can be applied even in the regime where shear motions are larger than turbulent motions.

(vii) We do not see strong effects, either in the ensemble-averaged statistical anisotropy, or scaling exponents, from magnetic fields. This is consistent with the fact that the saturation of the supersonic turbulent dynamo produces super-Alfvenic turbulence. However, we caution that the imposition of a sufficiently strong mean magnetic field (strong enough to make the turbulence sub-Alfvenic) could lead to different results.

(viii) For purposes of subgrid-scale models, our scalings imply that the "effective turbulent diffusivity" is not, in fact, a constant. However, if $\kappa \propto v_t(\ell)\ell$ for modes of wavelength ℓ, then sufficiently large wavelength modes $\ell \gg \Delta$ (where Δ is the simulation grid-scale) will always have their mixing resolved. Meanwhile since $v_t(\ell) \propto \ell^{\beta}$ with $\beta \sim 0.5 > 0$, the effect of unresolved, small-scale modes will be *dominated* by the largest un-resolved modes, i.e. those with $\ell \sim \Delta$. Therefore a scaling of the form typically adopted in Smagorinsky models is formally justified by our analysis, *provided* the following conditions are met: (a) the scale Δ lies *within the inertial range* of the turbulence, (b) the velocity compo-

nents identified by the shear tensor S are genuinely turbulent, and not some other (gravitational, outflow, inflow) motion, (c) the turbulence is statistically isotropic, and (d) shear is negligible on the scale Δ, as given by our note (vi) above. We stress that if any of these conditions is violated, the sense of the error will generally be that the Smagorinsky prescription *over-estimates* the diffusivity, potentially by very large factors. Moreover, we also emphasize that the constant pre-factor in such scalings must be calibrated to the appropriate definition of the grid scale Δ – this must be done independently for different numerical methods, because they have different "effective resolution scales" of the turbulent cascade, so we do not quote an effective value for it here.

We have focused on a simple, limited set of simulations illustrating some of the key turbulent processes controlling the diffusion of metals and other passive scalars in the ISM/CGM/IGM. Obviously, more detailed physical simulations including realistic phase structure and mixing by non-turbulent processes (e.g. galactic winds and fountains) will be necessary for a complete picture of mixing in realistic physical systems.

ACKNOWLEDGMENTS

Support for MJC was provided by the SURF program at Caltech and St John's College, Cambridge. Support for PFH & XM was provided by an Alfred P. Sloan Research Fellowship, NASA ATP Grant NNX14AH35G, and NSF Collaborative Research Grant #1411920 and CAREER grant #1455342. Support for JS was provided by the Sherman Fairchild foundation, and by the Gordon and Betty Moore Foundation through Grant GBMF5076 to Lars Bildsten, Eliot Quataert and E. Sterl Phinney. Numerical calculations were run on the Caltech compute cluster "Zwicky" (NSF MRI award #PHY-0960291) and allocation TG-AST130039 granted by the Extreme Science and Engineering Discovery Environment (XSEDE) supported by the NSF.

REFERENCES

Balakrishnan, V. 1985, Physica A: Statistical Mechanics and its Applications, 132, 569
Balescu, R. 1995, Physical Review E, 51, 4807
Banerjee, S., & Galtier, S. 2013, PhRvE, 87, 013019
Batchelor, G. K. 1949, Australian Journal of Scientific Research A Physical Sciences, 2, 437
Bauer, A., & Springel, V. 2012, MNRAS, 423, 2558
Boldyrev, S., Nordlund, Å., & Padoan, P. 2002, The Astrophysical Journal, 573, 678
Brandenburg, A., & Subramanian, K. 2005, PhysRep, 417, 1
del Castillo-Negrete, D., Carreras, B., & Lynch, V. 2005, Physical review letters, 94, 065003
Falkovich, G., Fouxon, I., & Oz, Y. 2010, Journal of Fluid Mechanics, 644, 465
Federrath, C., Klessen, R. S., & Schmidt, W. 2008, ApJL, 688, L79
Federrath, C., Roman-Duval, J., Klessen, R. S., Schmidt, W., & Mac Low, M.-M. 2010, A&A, 512, A81
Federrath, C., Schober, J., Bovino, S., & Schleicher, D. R. G. 2014, ApJL, 797, L19
Fujita, Y., Takizawa, M., & Sarazin, C. L. 2003, ApJ, 584, 190
Galtier, S., & Banerjee, S. 2011, Physical Review Letters, 107, 134501
Gioia, G., Lacorata, G., Marques Filho, E., Mazzino, A., & Rizza, U. 2004, Boundary-Layer Meteorology, 113, 187
Guan, X., & Gammie, C. F. 2008, ApJS, 174, 145
Hopkins, P. F. 2013, MNRAS, 430, 1653
—. 2015a, MNRAS, in press, arXiv:1509.07877
—. 2015b, MNRAS, 450, 53
Hopkins, P. F., & Lee, H. 2016, Monthly Notices of the Royal Astronomical Society, 456, 4174
Hopkins, P. F., & Raives, M. J. 2015, ArXiv e-prints
Ivezić, Ž., Beers, T. C., & Jurić, M. 2012, ARA&A, 50, 251
Klages, R., Radons, G., & Sokolov, I. M. 2008, Anomalous transport: foundations and applications (John Wiley & Sons)
Klessen, R. S., & Lin, D. N. 2003, PhRvE, 67, 046311
Kowal, G., & Lazarian, A. 2007a, in American Institute of Physics Conference Series, Vol. 932, Turbulence and Nonlinear Processes in Astrophysical Plasmas, ed. D. Shaikh & G. P. Zank, 421–430
Kowal, G., & Lazarian, A. 2007b, in Bulletin of the American Astronomical Society, Vol. 39, American Astronomical Society Meeting Abstracts, 984
Kritsuk, A. G., Lee, C. T., & Norman, M. L. 2013, Monthly Notices of the Royal Astronomical Society, stt1805
Kritsuk, A. G., Norman, M. L., Padoan, P., & Wagner, R. 2007a, ApJ, 665, 416
Kritsuk, A. G., Padoan, P., Wagner, R., & Norman, M. L. 2007b, in American Institute of Physics Conference Series, Vol. 932, Turbulence and Nonlinear Processes in Astrophysical Plasmas, ed. D. Shaikh & G. P. Zank, 393–399
Kritsuk, A. G., Wagner, R., & Norman, M. L. 2013, Journal of Fluid Mechanics, 729, 1
Kritsuk, A. G., et al. 2011, ApJ, 737, 13
Metzler, R., & Klafter, J. 2000, Physics reports, 339, 1
Monin, A. S., & Iaglom, A. M. 1975, Statistical fluid mechanics: Mechanics of turbulence. Volume 2 /revised and enlarged edition/
Pan, L., Padoan, P., & Kritsuk, A. G. 2009, Physical Review Letters, 102, 034501
Pan, L., & Scannapieco, E. 2010, ApJ, 721, 1765
Petit, A. C., Krumholz, M. R., Goldbaum, N. J., & Forbes, J. C. 2015, MNRAS, 449, 2588
Price, D. J., & Federrath, C. 2010, MNRAS, 406, 1659
Richardson, L. F. 1926, Proceedings of the Royal Society of London A: Mathematical, Physical and Engineering Sciences, 110, 709
Sawford, B. 2001, Annual review of fluid mechanics, 33, 289
Scannapieco, E., Schneider, R., & Ferrara, A. 2003, ApJ, 589, 35
Schmidt, W., Federrath, C., & Klessen, R. 2008, Physical Review Letters, 101, 194505
Schwarz, C., Beetz, C., Dreher, J., & Grauer, R. 2010, Physics Letters A, 374, 1039
Shen, S., Wadsley, J., & Stinson, G. 2010, MNRAS, 407, 1581
Shraiman, B. I., & Siggia, E. D. 2000, Nature, 405, 639
Smagorinsky, J. 1963, Monthly Weather Review, 91, 99
Springel, V. 2011, arXiv preprint arXiv:1109.2219
Stanislavsky, A. A. 2010, Astrophysics and Space Science Proceedings, 20, 63
Taylor, G. I. 1922, Proceedings of the London Mathematical Society, s2-20, 196
Tremonti, C. A., et al. 2004, ApJ, 613, 898
Wadsley, J. W., Veeravalli, G., & Couchman, H. M. P. 2008, MNRAS, 387, 427
Wagner, R., Falkovich, G., Kritsuk, A. G., & Norman, M. L. 2012, Journal of Fluid Mechanics, 713, 482
Yang, C.-C., & Krumholz, M. 2012, ApJ, 758, 48